Selective filter for SnO2 based gas sensors: application to hydrogen trace detection

Guy Tournier, Christophe Pijolat

SELECTIVE FILTER FOR SnO_2 BASED GAS SENSOR : APPLICATION TO HYDROGEN TRACE DETECTION

G.Tournier and C.Pijolat

Ecole Nationale Supérieure des Mines, Centre SPIN, LPMG-UMR 5148
158, Cours Fauriel, 42023 Saint-Etienne, France
email: tournier@emse.fr

ABSTRACT

The main drawback of the SnO_2 based gas sensors is their low selectivity. In this study, we present a highly selective hydrogen sensor with minimum cross sensitivity to ethanol, methane, carbon monoxide and hydrogen sulfide. Thick film SnO_2 sensors are treated by hexamethyldisiloxane (HMDS) at high temperature (500 – 600°C). After this treatment, the electrical properties of sensors are greatly modified: the sensitivity towards hydrogen is markedly increased and a high selectivity to hydrogen is achieved. In the meantime, transient responses curves to H_2 trace are altered: the response and recovery times are longer for treated sensors than for the untreated one. Nevertheless, if the temperature of the sensor is increasing from 450°C to 550°C, the response time notably decreases and the detection of hydrogen trace as low as 250 ppb v/v is quite possible with a good stability. HMDS treated material has been characterized with different analytical methods: SiO_2 formation is confirmed by Fourier transform infrared transmission spectroscopy (FTIR) and scanning electron microscopy (SEM) equipped with X probe. Moreover, temperature programmed desorption (TPD) experiments reveal that surface hydroxyl groups are involved in the HMDS- SnO_2 interaction. It could be supposed that a weakly porous Si based coating film overlaps the treated SnO_2 material and acts as a molecular sieve. Hydrogen can pass easily through the dense filter whereas the diffusion of other gases, and especially oxygen, is considerably reduced. The increase in sensitivity is explained with a simplified model based on an inversely proportional relation between the conductance of the SnO_2 material and the concentration of adsorbed oxygen ions.

Keywords: tin dioxide, silicon oxide, filter, hydrogen, selectivity.

I INTRODUCTION

Today hydrogen gas sensors are requested in several fields such as applications [1], fuel cell [2], radioactive waste storage and diverse safety problems due to the extremely explosive hydrogen gas. In other cases, hydrogen trace detection is required in order to evaluate a potential pollution. Among gas sensors, tin dioxide based semiconductor gas sensors are the most widely used for detection of inflammable or toxic gases. These sensors generally present a high sensibility and the detection of low levels of pollutants is quite possible. Nevertheless, the main drawback of this type of sensor is their lack of selectivity; for example, cross sensitivity to ethanol, carbon monoxide and methane prevents accurate hydrogen detection.

An approach to improve gas selectivity of a sensor includes the addition of a catalyst to the tin oxide powder. In the case of hydrogen gas sensors, good results are obtained with the use of silver [3] or palladium as additive. Another method is the use of a catalyst layer or a gas filter layer on the sensor surface. In our laboratory, several studies have already been performed on catalytic membranes [4,5]. With a platinum membrane, it is possible to enhance the methane selectivity of a sensor in presence of ethanol and carbon monoxide as interfering gases. In this study, we investigate the improvement of gas sensing properties of a thick film SnO_2 gas sensor by a SiO_2 coating film formed on the surface of the sensor. The dense layer of SiO_2 acts as a "molecular sieve", thereby the diffusion of gases with large molecular diameters was effectively controlled, resulting in a prominent selectivity for H_2 which presents a small molecular diameter. Several authors have already used a similar method in order to increase hydrogen selectivity of semiconductor-based sensors [6-11]. In several studies, the SiO_2 film is formed by a chemical vapour deposition (CVD) of silicone compounds [6, 7]. In the other cases, the improvement of gas-sensing properties of SnO_2 is achieved by surface chemical modification with ethoxysilanes compounds [8, 9]. Finally, a SnO_2 sensor in a SiO_2/SnO_2 double-layered structure could also be obtained by dipping or spin-coating methods by using a sol-gel process [10,11].

In our case, we investigate the improvement of gas sensing properties of a thick film SnO_2 gas sensor by a SiO_2 coating film formed by CVD deposition of hexametyldisiloxane (HMDS). This compound was thermally decomposed to SiO_2 on the hot sensor (working temperature around 500-600°C) resulting in a CVD dense layer on the surface of the SnO_2 material. The present study explores the effect of this SiO_2 layer on the electrical properties of the SnO_2 sensors. The influence of different treatment conditions (temperature, duration) on the response time, the sensibility and the selectivity towards hydrogen detection has been

studied. Characterization of untreated and SiO_2 modified SnO_2 material has been studied by different physical and chemical analysis:

X- ray diffraction (XRD) analysis, temperature-programmed desorption (TPD) experiments, Fourier transform infrared spectroscopy (FTIR) and scanning electron microscopy (SEM) equipped with X probe.

II EXPERIMENTAL

Preparation of SnO_2 sensors

SnO_2 thick films have been prepared by screen-printing technology. In this study, a semi-automatic Aurel C890 machine was used; the procedure for preparing material (ink composition, annealing temperature) has been described elsewhere [12]. The SnO_2 powder (Prolabo Company) is first mixed with a solvent and an organic vehicle without any mineral binder. An oxide film with a thickness of 20 microns is then deposited on an alpha-alumina substrate (38*5*0.4 mm^3) provided on one face with a screen-printed platinum heater and on the other face with two gold electrodes deposited by reactive sputtering. The SnO_2 material is finally annealed for12 hours at 700°C in air. Temperature and conductance of the obtained sensor are controlled with an electronic board that can be connected to a PC computer. Photography of this type of tin dioxide thick film sensor is shown in Fig. 1.

Formation of the SiO_2 coated film

SiO_2 thin film was grown by CVD deposition of HMDS on the surface of the SnO_2 material heated by the platinum heater of the sensor. The dry synthetic air carrier gas is bubbled into the HMDS liquid compound with a gaseous flow of 3 l/h under atmospheric pressure. The pressure of HMDS vapour, generated at room temperature, is about 6600 Pa (i.e. the saturated vapour pressure at 25° C) that corresponds to 6.5 % v/v concentration. Sensor temperature has been set between 500 and 600°C with a deposition time varying between 20 minutes and 6 hours. The monitoring of the electrical conductance of the sample during the HMDS treatment allows us to notice the different steps of the process. Before HMDS treatment, the sensor is placed under pure synthetic air flow at the treatment temperature in order to clean the SnO_2 surface; after the CVD deposition, the same operation is carried out in order to purge the bench of the residual HMDS vapour on one hand, and to estimate the reversibility of the electrical properties on the other hand. The scheme of the experimental installation is shown in Fig. 2.

Measurement of gas sensing properties

The sensors have been tested on a laboratory testing - bench by decreasing temperature from 500°C to 20°C in order to obtain the characteristic curves: sensor response versus

temperature. In our laboratory, these curves are generally plotted in order to estimate the selectivity of the sensors towards the different pollutant gases. In our case, the usual test pollutants are ethanol (50 ppm v/v), carbon monoxide (300 ppm v/v), methane (1000 ppm v/v) and hydrogen (500 ppm v/v) diluted in dry synthetic air. Gaseous flow has been set at 3 l/h.

On another testing - bench, isothermal experiments are carried out in order to estimate the transient response of the HMDS treated sensors to low levels of hydrogen (0 to 5 ppm v/v) in a mixture of argon and oxygen as carrier gas. For these studies corresponding to real experimental conditions, a high humidity level (R.H. $_{20°C}$ ≈ 90%) is required. A particular attention has been focused on the response and recovery times of the sensors. In this case, gaseous flow has been fixed at 4 l/h.

During these experiments, relative humidity and oxygen level have been monitored by using an hygrometer "Coreci" and a ceramic oxygen sensor "Pewatron", respectively.

Physico-chemical characterization of HMDS treated SnO_2 material

In order to determine if the SiO_2 coating film is crystallized or not, X-ray diffraction analysis of different samples (powdered or sintered SnO_2 material treated by HMDS) has been carried out on a Siemens D 5000 diffractometer.

The surface chemical modification of HMDS treated material have been investigated by temperature programmed desorption (TPD) experiments. A 10 mg sample (sintered or powdered material) is first annealed at 600°C for one hour in air. Then it is outgassed under high vacuum (in the order of 1 10^{-5} Pa) at ambient temperature in the thermodesorption apparatus; by means of a temperature-programmed furnace, the TPD run was carried out up to 900°C at a heating rate of 20°C min^{-1} in vacuum by monitoring desorbed gases with a mass spectrometer (Balzers). Adsorbed oxygen species (O^- or O^{2-}) and surface hydroxyl groups have been particularly examined.

FTIR transmission spectra of HMDS treated SnO_2 powder were recorded on a BIORAD FTS 185 FT-IR spectrometer using attenuated total reflection (ATR) in a diamond crystal.

Cross-sectional views of untreated and HMDS treated material (thick film or sintered pellet) were observed by scanning electron microscopy (SEM) on a JEOL JSM 840.

III RESULTS

Electrical results

During HMDS treatment, different steps could be distinguished by continuous monitoring of the conductance of the sensor. For example, Fig. 3 shows the evolution of the response sensor at 600°C: in a first step, the conductance markedly increases from 1 10^{-4} S to

$2\ 10^{-3}$ S (20 times); in a second step, the sensor signal decreases and is not yet stabilized after 4 hours. Moreover, the value of the maximum of the conductance increases with the treatment temperature (in the range 450-600°C). Different treatment times have been investigated between 20 minutes and 6 hours. The longer the deposition time is, the smaller the final conductance value is. In this case (long time treatment), the recovery time in pure air is very long when HMDS is removed.

The characteristic curves of conductance versus temperature are shown in Fig. 4 for unmodified and HMDS treated SnO_2 gas sensor. Before treatment (Fig. 4 a), the sensitivities (for previously mentioned concentrations) measured at 500°C and defined by the ratio $(G-G_0)/G_0$, where G is the conductance under gas and G_0 the conductance under pure air, vary between 5 and 20 in all cases (see Fig. 5). After a HMDS treatment at 600°C for 6 hours (Fig. 4 b), the sensitivities to C_2H_5OH, CO and CH_4 are drastically reduced near 0 all over the temperature range; on the contrary, the H_2 sensitivity is markedly increased and reaches 170 at 500°C (see Fig. 5). The initial non-selective sensor is modified into a H_2 selective sensor with the HMDS treatment. When the time treatment is decreasing (for example from 6 hours to 20 minutes) or if temperature is less than 600°C (for example 450°C or 500°C), the effects are less pronounced but the H_2 sensitivity and selectivity remain high; the results concerning a sensor treated for 6 hours at 500°C are shown in Fig. 6.

In another set of experiments, hydrogen trace detection has been evaluated under particular experimental conditions in argon as carrier gas. The oxygen concentration and the relative humidity measured at 20°C have been fixed respectively at 5% v/v and 90%. Fig. 7 shows the 5 ppm v/v hydrogen response, measured at the 450°C usual temperature, of untreated and different HMDS treated SnO_2 sensors. It is clear that the HMDS treatment improve the hydrogen response as the sensitivity to 5 ppm v/v hydrogen is varying from 0.8 for the untreated sensor to 2.5 and higher than 10 for the sensors treated by HMDS for 6 hours at 500°C and 600°C, respectively. On the contrary, the response time and also the recovery time are longer (particularly in the case of the 600°C treatment) for treated sensors than for the untreated one. The detection of H_2 trace is then seriously impeded. Nevertheless, if the temperature of the sensor is increased, the response time decreases and the detection of H_2 concentration as low as 250 ppb v/v is quite possible, as it is shown in Fig. 8 in the case of an operating temperature of 550°C. Moreover, Fig. 9 shows the good stability of the 250 ppb v/v H_2 response at 550°C of a sensor treated 4 hours at 600°C by HMDS. Another way to improve the response time is to reduce the duration of the treatment; nevertheless it could be observed

only a slight effect when the treatment time varies between 0.3 h and 6 h in the case of a HMDS treatment carried out at 600°C.

Without H_2 pollutant, on exchanging dry O_2 (5% v/v) in argon for dry argon and reverse, it could be observed that the response of a HMDS treated sensor was considerably slowed down in comparison with the untreated one, as shown in Fig. 10.

Finally, no serious influence of hydrogen sulfide (H_2S) as interfering gas could be observed on HMDS treated sensors when an irreversible effect, especially in a wet atmosphere, usually affects the untreated material. As shown in Fig.11, no response for H_2S concentrations (in the range 0 – 1 ppm v/v) could be detected with a 600°C treated sensor.

Samples characterization

Different samples have been studied by X-ray diffraction analysis. Whatever the treatment temperature in the range 400-500°C is, HMDS treated SnO_2 powder shows no chararacteristic pattern of the SiO_2 structure, while Si could be detected by MEB analysis with X probe (see hereafter). Even if the treatment is carried out at 600°C for 24 hours, no well-defined peak could be distinguished. In order to verify if the SiO_2 material is masked by the preponderant SnO_2 phase, a pure alumina substrate (without SnO_2 material) have been treated during a long time by HMDS at 600°C and no SiO_2 trace could be detected. Nevertheless, in this case, grazing incidence measurement could be undoubtedly more suitable for our purpose. Finally, a powder obtained by thermally decomposition in a furnace at 500°C of HMDS vapour has been examined by XRD: only weak and not well-defined peaks could be detected and they could not be attributed to a well-established structure.

TPD experiments are carried out on powdered or sintered materials. In fact, the results are the same for the two kinds of sample. In these experiments, three temperatures of treatment have been chosen (i.e. 400°C, 450°C and 500°C), the duration being set at 0.5 hour. Fig 12 shows the TPD spectra of water (m/e = 18) and oxygen (m/e = 32) in the case of pure and HMDS treated SnO_2 powder. These species could be correlated with hydroxyl groups (OH) and ionosorbed oxygen (O^- or O^{2-}) adsorption sites respectively. In the case of untreated material, surface hydroxyl groups desorb between 100°C and 500°C with a sharp maximum desorption peak around 350°C (see Fig. 12 a). On the contrary, whatever the HMDS temperature treatment belonging the range 400°C-500°C, the desorption spectrum intensity is considerably reduced and three weak peaks could be observed near 200°C, 350°C and 600°C**,** respectively (see Fig. 12 a). Moreover, the intensity of the 200°C peak decreases and conversely the 600°C peak intensity increases when the HMDS temperature treatment varies from 400°C to 500°C.

Fig. 12 b shows the desorption spectra of oxygen for the same samples as previously. For the untreated material, three desorption peaks could be observed with maxima situated at 600°C, 750°C and 875°C**,** respectively. In the case of HMDS treated samples, it is observed that the magnitude of desorption signal strongly decreases for temperature higher than 500°C, in correlation with the disappearance of all the peaks above-mentioned.

Fig. 13 shows FTIR transmission spectra obtained for untreated and HMDS treated SnO_2 powdered samples. These spectra are characterized by several absorption bands: one of the principal bands is a peak centered at 615 cm^{-1} that could be assigned to a fundamental vibration ν(Sn-O) of tin dioxide [13]. In the case of 30 minutes HMDS treated samples, new absorption bands could be observed near 1090 cm^{-1} and 815 cm^{-1}. The intensity of these bands increases when the treatment temperature increases from 400°C to 500°C. Moreover, the absorption spectrum obtained for the powder resulting of HMDS thermal decomposition at 500°C is reported on the same graph: it could be observed that the bands situated at 1090 cm^{-1} and 815 cm^{-1} are also present but their intensity is very large. These absorption bands could be assigned to the vibration modes of Si-O-Si, stretching mode around 1090 cm^{-1} and bending mode around 820 cm^{-1} [14].

Fig. 14 shows scanning electron microscope (SEM) cross-sectional images for untreated and 24 hours 600°C HMDS treated thick films SnO_2. In Fig.14 a it could be observed that untreated material present an average particle size in the order of 0.1 to 0.3 micron; moreover, porosity of the thick film is clearly visible on the graph. In the case of HMDS treated sample, the morphology of the SnO_2 material is greatly modified as shown in Fig. 14 b: on one hand, a grain growth could be observed since particle size is higher than 0.5 – 0.6 micron; on the other hand, the particles seem to be overlapped by a quasi continuous film with very low porosity. In fact, it could be suggested that a real paste has been deposited on the thick film, which induces a more compact surface aspect than the untreated sample. If the observed grain growth is only due to the SiO_2 film formation, the thickness of this layer could be roughly estimated in the range 0.1 to 0.25 micron. Moreover, X probe analysis has been performed on HMDS treated thick film. In the studied volume sample, i.e. one cube micrometer, silicon concentration has been estimated to 6-weight % (that corresponds with 20 atomic %), the other elements being tin and oxygen.

IV DISCUSSION

During the interaction between HMDS and SnO_2 material, two steps could be observed (see Fig. 3). In the beginning, the HMDS decomposition at the SnO_2 surface induces an electrical signal, which is represented by an increase of the conductance of the sensor as it is

observed with all reducing gases. It could be supposed that surface hydroxyl groups, which are strongly modified after HMDS treatment, are involved in this reaction (see Fig. 12 a). In a second step, after the maximum of conductance has been reached, the sensor signal diminishes; during this period, the HMDS decomposition continues and a silicon based compound is elaborated as revealed by X probe results. On one hand, this compound is probably a silicon dioxide material because absorption bands, assigned to Si-O-Si bonds, have been observed during FTIR spectra analysis (see Fig. 13). On the other hand, this silica compound is not well crystallised (or amorphous) as no well-defined peaks could be distinguished by X-ray diffraction analysis. The reaction then progresses by HMDS decomposition on the SiO_2 already grown without any electrical effect on the SnO_2 conductance; nevertheless, the thickness of the insulating layer increases and then induces a decrease of the conductance of the sensor. The longer the deposition time is, the smaller the final value of the conductance is. When the HMDS is removed, the conductance decreases again because the re-adsorption of oxygen gas, as it could be usually observed in the case of reversible adsorption. Nevertheless, the recovery time is longer and the amplitude of the recovery is smaller for a long time treated sensor than for a short time treated one. Moreover, the recovery is only partial; consequently, HMDS treatment induces an irreversible effect.

At the beginning of the treatment, the SiO_2 material is probably grown up around each SnO_2 particle. As the process is pursued, a quasi-continuous dense layer of SiO_2 is finally obtained, as it could be observed on SEM images (see Fig. 14 b). This not very porous film is thus able to work as a molecular sieve. Among the different gases considered, hydrogen, which presents the smallest molecular diameter (0.22 nm) [7,15], can easily pass through the dense SiO_2 surface layer. On the contrary, the biggest molecules like oxygen (0.30 nm), carbon monoxide (0.38 nm) or methane (0.38 nm) are diffusion – controlled by the SiO_2 film. The hydrogen sensitivity and selectivity are then strongly improved compared with the untreated sensor as it can be seen on Fig. 4, 5 and 6. As another example, no significant response under H_2S has been observed with HMDS treated sensors (see Fig. 11) whereas the untreated sensor is usually subjected to an irreversible effect.

However, as it has been indicated by several authors [7-9,11], the response and recovery times are greatly affected by HMDS treatment, especially in the case of low hydrogen concentration (see Fig. 7). Concerning the response time, it could be supposed that SiO_2 film is too dense, so the diffusion speed from the atmosphere to the inner region of the hydrogen molecule, despite its small size, is slowed down. The recovery time, when H_2 is removed, is directly related to the progressive re-adsorption of O_2 molecules; as it could be observed on

Fig. 10, the kinetics of adsorption and desorption of oxygen are considerably reduced when the SiO_2 layer has been deposited on the SnO_2 material. This phenomenon is undoubtedly due to the large molecular diameter of O_2 molecule. If the temperature of the treatment is diminished, the SiO_2 filter is thinner and probably less compact, so the response and recovery times could be improved, as it could be seen in Fig. 7. In this graph, the electrical performances of the untreated, 500°C and 600°C HMDS treated sensors have been compared. The kinetic response of the 500°C treated sensor is considerably faster than that of the 600°C treated one and the H_2 sensitivity remains high: the sensitivity for 5 ppm v/v H_2 is about 2.5 when it is 0.8 in the case of the untreated sensor. In any case, the good performances of the sensor, especially the high hydrogen selectivity, are less pronounced when the response and recovery times have been improved (compare Fig. 4 b with Fig. 6 b, for the 6 hours 600°C and 500°C HMDS treated sensors respectively). Another way to reduce the response time is of course to increase the operating temperature of the sensor (for example from 450°C to 550°C). In these conditions, the response time is reasonable and hydrogen traces as low as 250 ppb v/v could be detected with a good stability (see Fig. 8 and Fig. 9).

As shown in Fig. 12 b, the three desorption peaks of O_2 observed on untreated SnO_2, with maxima situated around 600°C, 750°C and 875°C, have been almost completely disappeared on HMDS treated material. The "low temperature" peaks (i.e. 600°C and 750°C in our case) could generally be ascribed to some oxygen species adsorbed on SnO_2 (O^- or O^{2-}) whereas the "high temperature" peak (i.e. 875°C in our case) is likely to be the dissociation of a part of lattice oxygen [8,16]. It could be reasonably supposed that adsorbed oxygen species are less numerous on HMDS treated SnO_2 material and could not be observed with this analytical method, that agree with the fact that oxygen diffusion through the SiO_2 film is impeded. In the same manner, the desorption of lattice oxygen is considerably reduced at high temperature; this may confirm that the surface of SnO_2 particles are completely covered with a SiO_2 film.

These results suggest several remarks. On one hand, the improvement of the hydrogen selectivity with the SiO_2 filter is quite comprehensible if we take into account the small diameter of the hydrogen molecule among the other considered gases. On the other hand, the increase in sensitivity is more difficult to explain. In fact, the conductivity of the tin dioxide is usually governed by a steady concentration of the adsorbed oxygen ions, which is determined by chemical dynamics including oxidation and diffusion reactions [7]. Under oxygen based carrier gas, the concentration of adsorbed oxygen ions on the HMDS treated sensor is lower than those on the untreated one (as previously mentioned); when hydrogen reacts with these species, the conductance greatly increases on treated sensor like the re-adsorption of oxygen

molecules (inducing, on the contrary, a decrease in conductance) is considerably slowed down. Then, the high conductance value obtained at the stationary state, due to a low steady concentration of adsorbed oxygen ions, induces an interesting high sensitivity to hydrogen (see Fig. 5). This result is the same when oxygen concentration in the carrier gas is reduced [17,18]: in the case of a pure SnO_2 sensor, the number of surface adsorbed oxygen ions decreases when the oxygen partial pressure in the carrier gas decreases, and the gas (hydrogen or methane) sensitivity is consequently high. It is possible to explain this phenomenon by using the usually admitted mechanism described hereafter [19]:

The two reactions that take place are as follows:

-adsorption of oxygen on a site s of SnO_2:

$$\tfrac{1}{2}\, O_2 + e^- + s \underset{k_{-1}}{\overset{k_1}{\rightleftharpoons}} s\text{-}O_{ads}^- \quad (1) \quad \text{with} \quad K = k_1/k_{-1}$$

(where k_1 and k_{-1} denote the rate constant for the direct and the reverse reaction, respectively)

removing electrons from the conduction band, and as a consequence, decreasing the conductance G.

- reaction of reducing gas (R) with adsorbed oxygen:

$$R + s\text{-}O_{ads}^- \xrightarrow{k_2} RO \longrightarrow + e^- + s \quad (2)$$

(where k_2 is the rate constant)
releasing electrons in the conduction band, and as a consequence, increasing the conductance G.

Under oxygen based carrier gas, only reaction (1) is concerned and at the stationary state, the O^- concentration ($[O^-]_0$) is linked to the fraction of surface coverage θ_0 and could be expressed by Eq. (3), according to the Langmuir adsorption law:

$$\theta_0 = \frac{K\, P_{O_2}^{1/2}}{1 + K\, P_{O_2}^{1/2}} = \alpha\, [O^-]_0 \quad (3) \ (\text{K previously defined})$$

where α and P_{O_2} are a constant and the partial pressure of oxygen; respectively.

When the gas R is present, Eq. (1) and (2) have to be considered and, at the stationary state, we can write:

$$d[\theta]/dt = 0 = k_1 P_{O_2}^{1/2} (1-\theta_g) - k_{-1} \theta_g - k_2 P_g \theta_g \qquad (4)$$

where P_g and θ_g are respectively the partial pressure of gas and the fraction of surface coverage of O^- species.

From Eq. (4), it is possible to calculate θ_g by the following formula:

$$\theta_g = \frac{k_1 P_{O_2}^{1/2}}{k_{-1} + k_2 P_g + k_1 P_{O_2}^{1/2}} = \alpha [O^-]_g \qquad (5)$$

where $[O^-]_g$ is the O^- concentration under gas.

As it has been above mentioned, the conductance G of the SnO_2 sensor is correlated with the adsorbed oxygen ions concentration: higher this concentration is, smaller the conductance value is and reverse. According to the assumption, as made by Advani et**.** al. [20], that the relation, between the conductance and the oxygen ions concentration $[O^-]$, is roughly estimated by the formula:

$$G \approx k / [O^-] \qquad (6)$$

where k is a constant, the response represented by the sensitivity S could be defined by the following formula:

$$S = \frac{G_g - G_0}{G_0} = G_g / G_0 - 1 = [O^-]_0 / [O^-]_g - 1 = \theta_0 / \theta_g - 1 \qquad (7)$$

where G_g and G_0 are the conductance values in specific gas ambient and oxygen based carrier gas, respectively.

Eq. (6) is only valid for $[O^-] \neq 0$, i.e. only with oxygen based carrier gas. Moreover, in the case of HMDS treated sensors, the dense SiO_2 filter is sufficiently porous to allow the slow diffusion through the film of oxygen molecules and adsorption of them on the SnO_2 surface.

From Eq. (3), (5) and (7), it could be written:

$$S = \left(\frac{K P_{O_2}^{1/2}}{1 + K P_{O_2}^{1/2}} * \frac{k_{-1} + k_2 P_g + k_1 P_{O_2}^{1/2}}{k_1 P_{O_2}^{1/2}} \right) - 1 \qquad (8)$$

As $K = k_1/k_{-1}$, the sensitivity S could be expressed as:

$$S = \left(1 + \frac{k_2 Pg}{k_{-1} + k_1 P_{O_2}^{1/2}} \right) - 1 = \frac{k_2 Pg}{k_{-1} + k_1 P_{O_2}^{1/2}} \qquad (9)$$

From Eq. (9) and for a constant gas partial pressure, the sensitivity S increases when the oxygen partial pressure decreases that is to say when the ionosorbed oxygen concentration diminishes (see Eq. 1). With a HMDS treated sensor, the SiO_2 layer induces a smaller steady concentration of adsorbed oxygen ions than in the case of the pure SnO_2 sensor: this phenomenon is analogous with a decrease of oxygen partial pressure in the gaseous flow. Moreover, the hydrogen partial pressure near the SnO_2 surface is practically the same in the two types of SnO_2 sensors**.** As a consequence, the modified sensor present a higher hydrogen sensitivity than the unmodified one. This interpretation is only based on a simplified model: other parameters ought to be taken into account, in particular the possible presence of adsorbed hydroxyl groups (OH^-) due to the interaction of water with tin dioxide surface. This water could be present in a wet atmosphere or formed during the oxidation of the reducing gas (hydrogen as for example) on the SnO_2 material.

V CONCLUSIONS

In this study, the modifications of the electrical performances of thick film SnO_2 gas sensors by hexamethyldisiloxane (HMDS) treatment have been studied. A Si based thin film has been formed by CVD deposition of HMDS at high temperature (500°C or 600°C). Each SnO_2 particle is then coated by a SiO_2 layer with very low porosity and consequently, this film acts as a molecular sieve.

On one hand, hydrogen, which has the smallest molecule size among the different considered gases i.e. carbon monoxide, methane, ethanol and hydrogen sulfide, can pass easier than the other gases through the dense filter. A prominent selectivity for hydrogen detection is then achieved. On the other hand, because of the large diameter of oxygen molecules, adsorbed oxygen ions are not very numerous on HMDS treated tin dioxide surface that induces an increase of hydrogen sensitivity with regard to the electrical performances of the untreated sensor. This phenomenon is explained by taking into account that the conductivity of tin dioxide is governed by the steady concentration of the adsorbed oxygen ions; a simplified

model based on an inversely proportional relation between the conductance and the oxygen ions concentration has been developed.

In the meantime, the response and recovery kinetics of sensors are considerably reduced by the HMDS treatment. In consequence, it seems to be necessary to raise the operating temperature of the sensor from the usual one i.e. 450°C to 550°C for example. Under these working conditions, hydrogen concentrations as low as 250 ppb could be detected with good electrical results (sensitivity and stability). Another way to reduce the response time is to control the HMDS effects by decreasing the duration and / or the temperature of the treatment, but to the detriment of hydrogen sensitivity and selectivity.

Current experiments are performed in order to obtain the best compromise between high hydrogen detection performances (sensitivity and selectivity) and reasonable response and recovery times to use these hydrogen sensors in special industrial applications.

References

[1] C.Pijolat, G.Tournier, P.Breuil, D.Matarin and P.Nivet, Hydrogen detection on a cryogenic motor with a SnO_2 sensors network, Sens. Actuators, B, Chem 82 (2002) pp. 166-175.

[2] N.Q.Minh, Ceramic fuel cells, J.Am.Ceram.Soc., 76(3) (1993) pp 563-588.

[3] N.Yamazoe, Y.Kurokawa and T.S Seiyama, Hydrogen sensitive gas detector using silver added tin (IV) oxide, Chemistry Letters, (1982) pp 1899-1902.

[4] P.Montmeat, C.Pijolat, B.Rivière, G.Tournier and J.P.Viricelle, Effect of a platinum membrane on the sensing properties of materials based on thin and thick tin dioxide films, Materials Science and Engineering, C 21 (2002) pp 113-123.

[5] P.Montméat, C.Pijolat, B.Rivière, G.Tournier and J.P.Viricelle, The influence of a platinum membrane on the sensing properties of a tin dioxide thin film, Sens. Actuators, B, Chem 84 (2002) pp 148-159.

[6] K.Fukui and K.Komatsu, H_2 gas sensor of sintered SnO_2, Pro. Int. Mtg. on Chemical Sensors, Fukuoka, Japan, (1983) pp 52-56.

[7] A.Katsuki and K. Fukui, H_2 selective gas sensor based on SnO_2, Sens. Actuators, B, Chem 52 (1998) pp 30-37.

[8] K.Wada and M.Egashira, Improvement of gas-sensing properties of SnO_2 by surface chemical modification with diethoxydimethylsilane, Sens. Actuators, B, 53 (1998) pp 147-154.

[9] K.Wada and M.Egashira, Hydrogen sensing properties of SnO_2 subjected to surface chemical modification with ethoxysilanes, Sens. Actuators, B, Chem 62 (2000) pp 211-219.

[10] K.Wada and M.Egashira, Improvement of gas-sensing properties of a Pd/SnO_2 sensor by SiO_2 coating films formed by dipping method, Journal of the Ceramic Society of Japan, Int.Edition, 106 (1998) pp 86-90.

[11] C.D.Feng, Y.Shimizu and M.Egashira, Effect of gas diffusion process on sensing properties of SnO_2 thin film sensors in a SiO_2/SnO_2 layer-built structure fabricated by sol-gel process, J.Electrochem.Soc., 141 (1) (1994) pp 220-225.

[12] B.Rivière, J.P.Viricelle and C.Pijolat, Micro-machined tin oxide gas sensors manufactured in screen-printing technology, Sens. Actuators, B, Chem 93 (2003) pp 531-537.

[13] D.Amalric-Popescu and F.Bozon-Verduraz, Infrared studies on SnO_2 and Pd/SnO_2, Catalysis Today, 70 (2001) pp 139-154.

[14] M.T.Kim, Deposition kinetics of silicon dioxide from tetraethylorthosilicate by PECVD, Thin Solid Films, 360 (2000) pp 60-68.

[15] J.W. Moore, Physical Chemistry, (1973) Table 7.5.

[16] N. Yamazoe, J. Fughigami, M. Kishikawa and T. Seiyama, Interactions of tin oxide surface with O_2, H_2O and H_2, Surface Science, 86 (1979) pp 335-344.

[17] G.S.V.Coles, G.Williams and B.Smith, The effect of oxygen partial pressure on the response of tin (IV) oxide based gas sensors, J.Phys.D: Appl. Phys., 24 (1991) pp 633-641.

[18] G.Tournier and C.Pijolat, Influence of oxygen concentration in the carrier gas on the response of tin dioxide sensor under hydrogen and methane, Sens. Actuators, B, Chem 61 (1999) pp 43-50.

[19] S.Morrison, Selectivity in semiconductor gas sensors, Sens. Actuators, 12 (1987) pp 425-440.

[20] G.N.Advani and A.G. Jordan, Thin films of SnO_2 as solid state gas sensors, Journal of Electronic Materials, 9(1) (1980) pp 29-49.

FIGURES LEGENDS

Fig. 1: Photography of a SnO_2 thick film sensor
(a): view of the front side (SnO_2 based material); (b) : view of the reverse side (Pt heater);
(c) view of the entire sensor

Fig. 2: Scheme of the experimental apparatus for CVD deposition of SiO_2 on a SnO_2 thick film sensor

Fig. 3: Response curve of a SnO_2 thick film sensor to 6.5 % v/v HMDS in dry synthetic air at 600°C

Fig. 4: Characteristic curves of conductance vs. temperature under different diluted gases in dry synthetic air for a SnO_2 thick film sensor
(▲) : C_2H_5OH (50 ppm v/v); (■): CO (300 ppm v/v); (Δ): CH_4 (1000 ppm v/v);
(□): H_2 (500 ppm v/v); (●): dry synthetic air
(a): untreated; (b): after 6 hours - 600°C HMDS treatment

Fig. 5: Influence of a 6 hours 600°C HMDS treatment on gases sensitivities measured at 500°C of a SnO_2 thick film sensor

Fig. 6: Characteristic curves of conductance vs. temperature under different diluted gases in dry synthetic air for a SnO_2 thick film sensor
(▲) : C_2H_5OH (50 ppm v/v); (■): CO (300 ppm v/v); (Δ): CH_4 (1000 ppm v/v);
(□): H_2 (500 ppm v/v); (●): dry synthetic air
(a): untreated; (b): after 6 hours - 500°C HMDS treatment

Fig. 7: Transient response curves to 5 ppm v/v H_2 at 450 °C of three SnO_2 thick film sensors
Carrier gas: 5 % v/v O_2 in argon; R.H. (20°C) # 90%; S = sensitivity

Fig. 8: Transient response curves to 0.25, 1, and 5 ppm v/v H_2 at 550°C of two HMDS treated SnO_2 thick film sensors
Carrier gas: 5 % v/v O_2 in argon; R.H. (20°C) # 90%

Fig. 9: Stability of the response to 0.25 ppm v/v H_2 at 550°C for a 4 hours 600°C HMDS treated SnO_2 thick film sensor
Carrier gas: 5 % v/v O_2 in argon; R.H. (20°C) # 90%

Fig. 10: Response at 550°C of a 6 hours 600°C HMDS treated SnO_2 thick film sensor on exchanging dry argon for dry argon with 5 % v/v O_2 (a) and reverse (b)

Fig. 11: Response to 0.25, 0.5, 0.75, and 1 ppm v/v H_2S at 450°C of a 6 hours 600°C HMDS treated SnO_2 thick film sensor
Carrier gas: 5 % v/v O_2 in argon; R.H. (20°C) # 90%

Fig. 12: TPD spectra for untreated and HMDS treated SnO_2 powder
(a) water (m/e = 18); (b): oxygen (m/e = 32)

Fig. 13: FTIR transmission spectra of untreated and HMDS treated SnO_2 powder; spectrum of a powder resulting from HMDS decomposition at 500°C is also visible on the graph
Method: attenuated total reflection (ATR) in a diamond crystal

Fig. 14: Scanning electron microscope (SEM) cross-sectional images of SnO_2 thick films
(a): untreated; (b): 24 hours 600°C HMDS treated

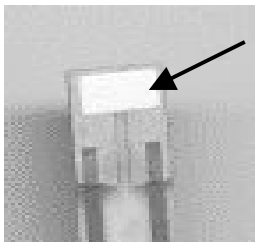

SnO_2 based material

(a)

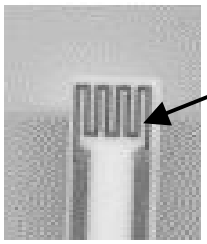

Pt heater

(b)

(c)

Fig. 1

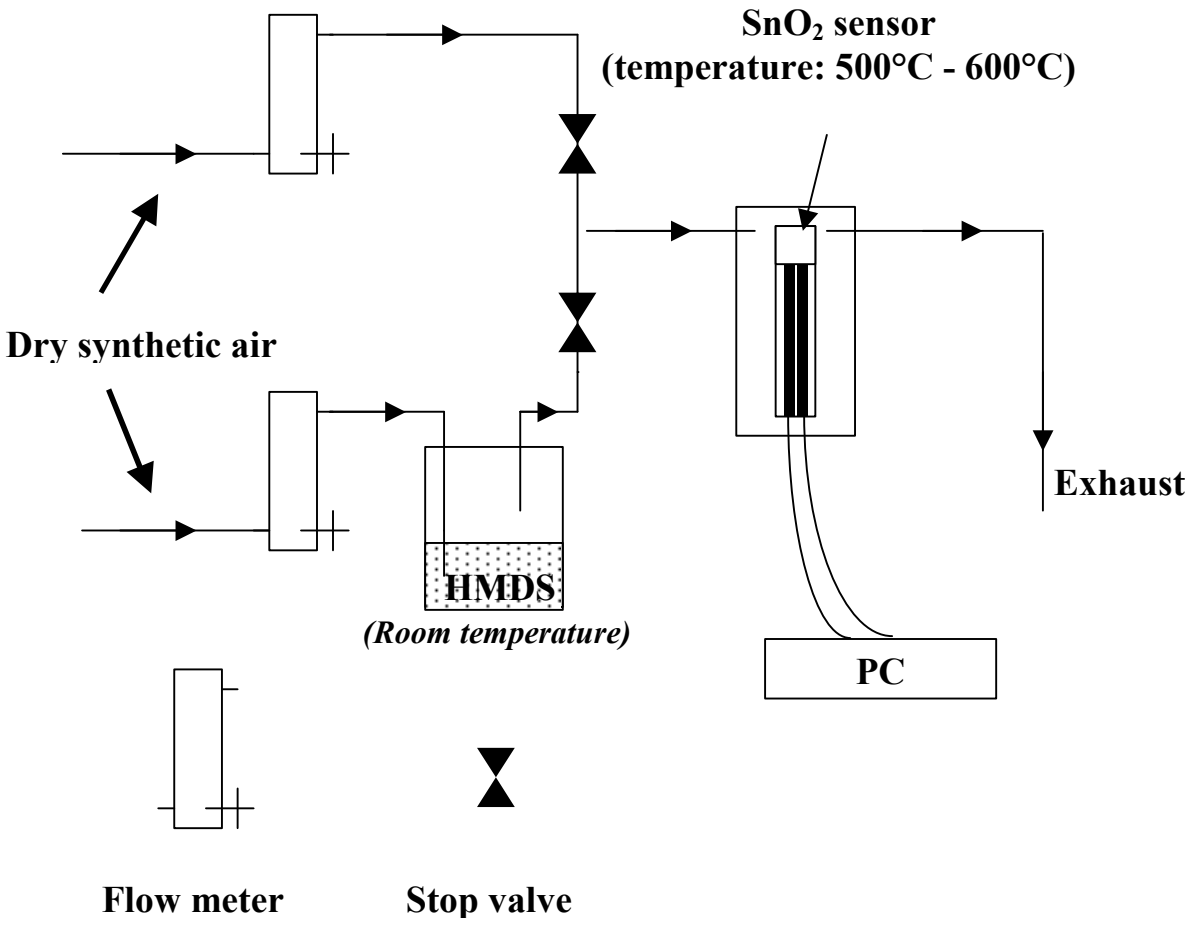
SnO2 sensor
(temperature: 500°C - 600°C)
Dry synthetic air
HMDS
(Room temperature)
Exhaust
PC
Flow meter
Stop valve

Fig. 2

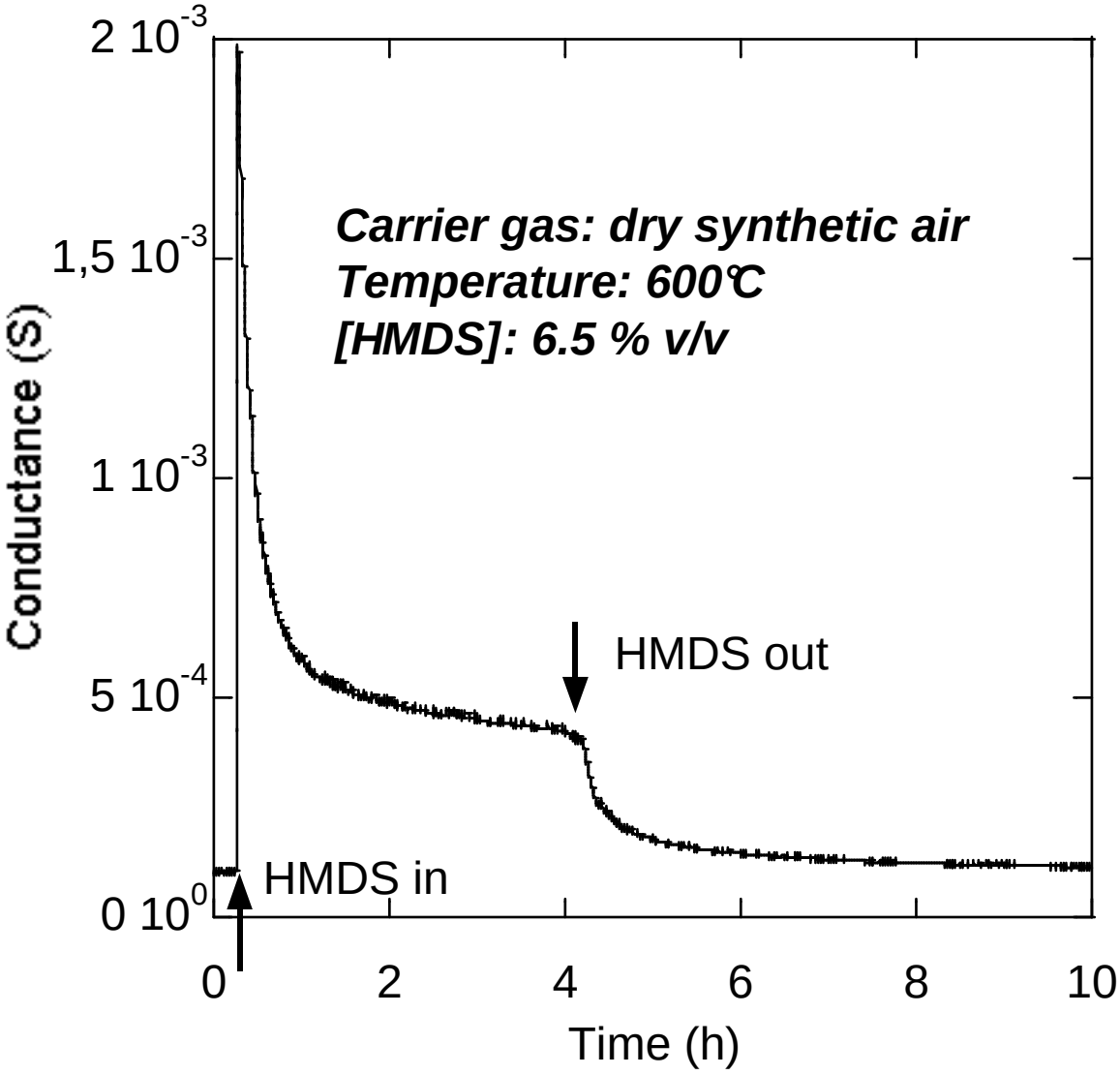
2 10-3
1,5 10-3
1 10-3
5 10-4
0 100
Conductance (S)
Carrier gas: dry synthetic air
Temperature: 600℃
[HMDS]: 6.5 % v/v
HMDS out
HMDS in
0
2
4
6
8
10
Time (h)

Fig. 3

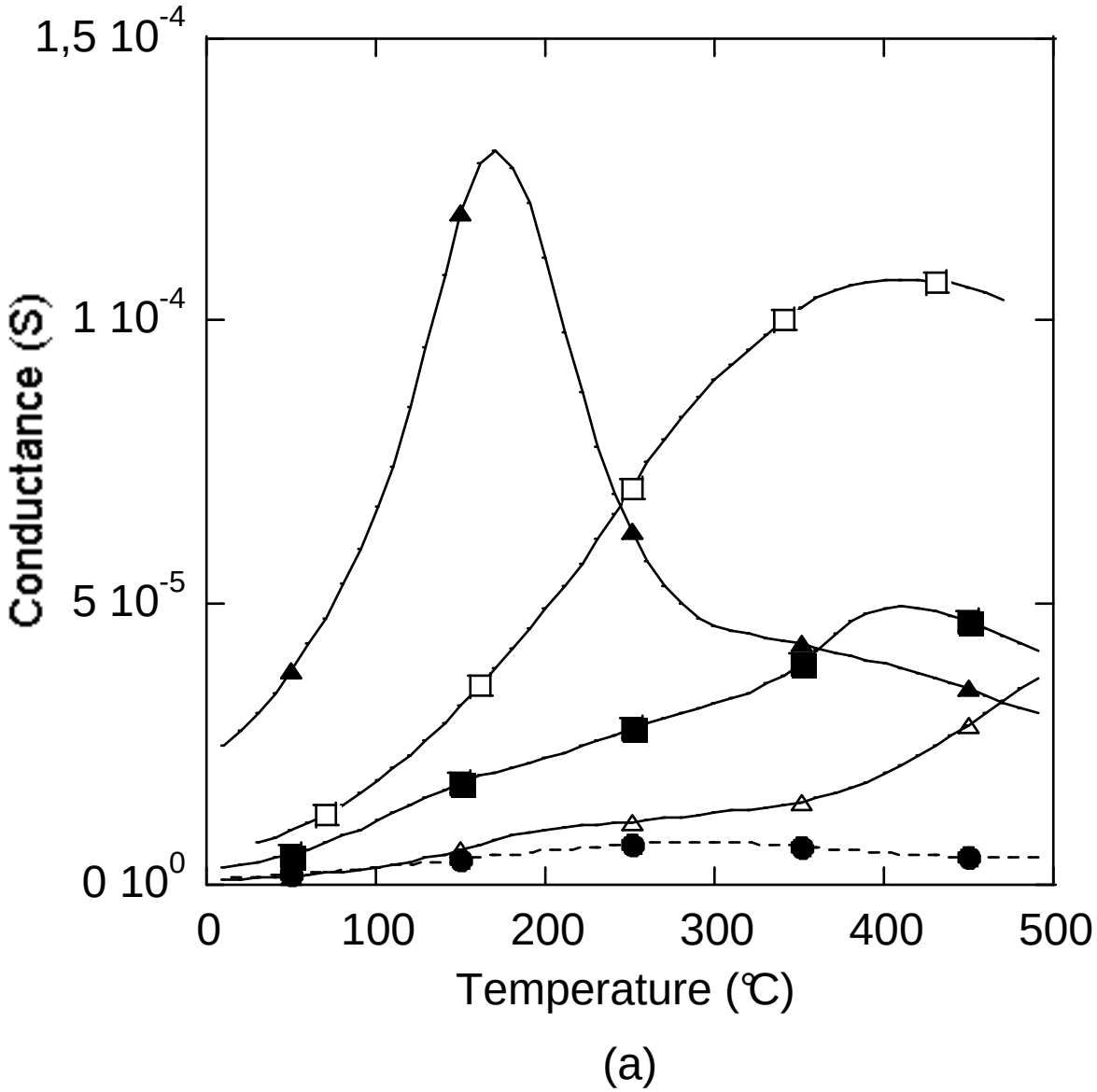
1,5 10-4
1 10-4
5 10-5
0 100
Conductance (S)
0
100
200
300
400
500
Temperature (℃)
(a)

Fig. 4 a

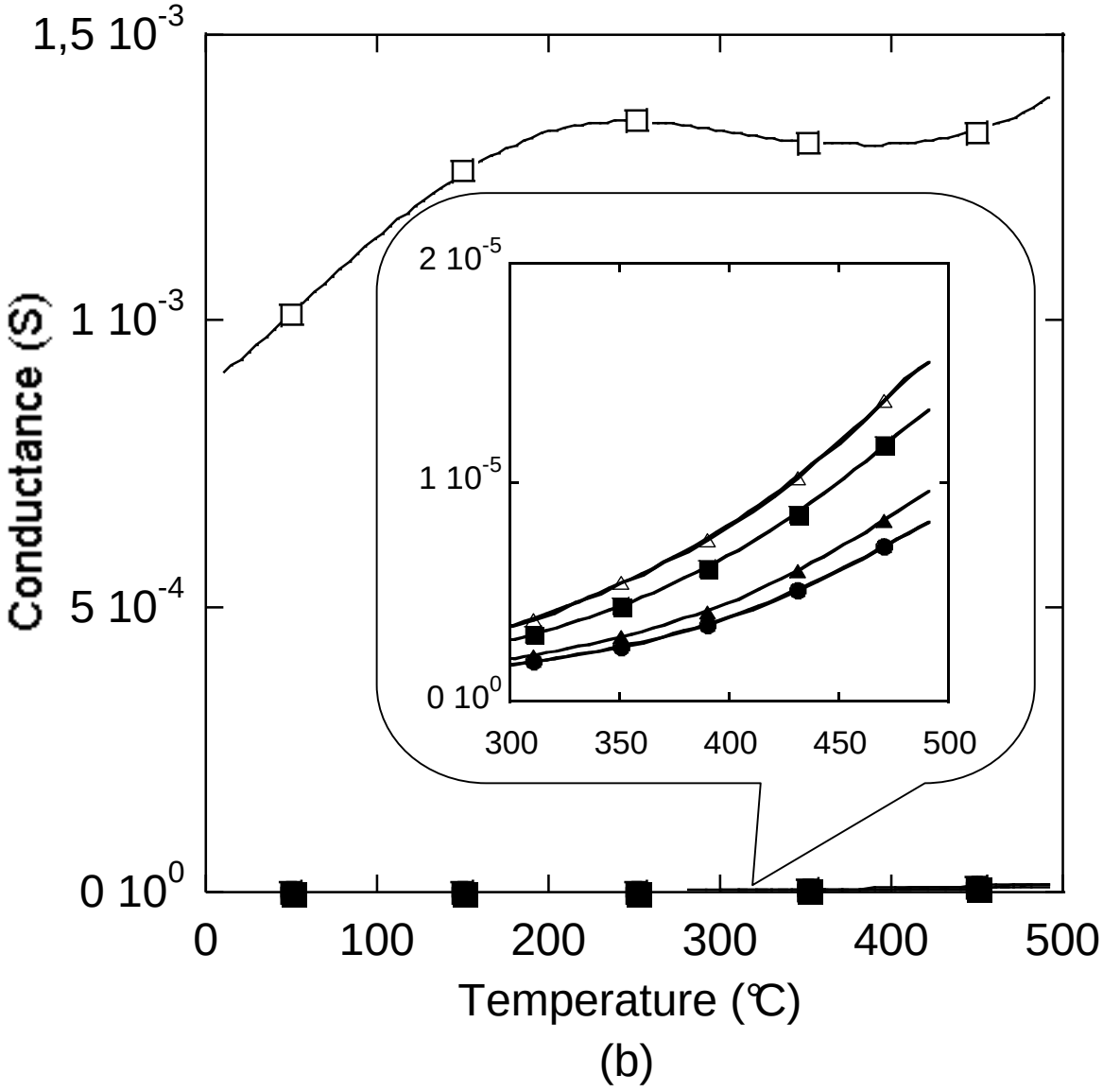
1,5 10-3
1 10-3
5 10-4
0 100
Conductance (S)
0
100
200
300
400
500
Temperature (℃)
(b)
2 10-5
1 10-5
0 100
300
350
400
450
500

Fig. 4 b

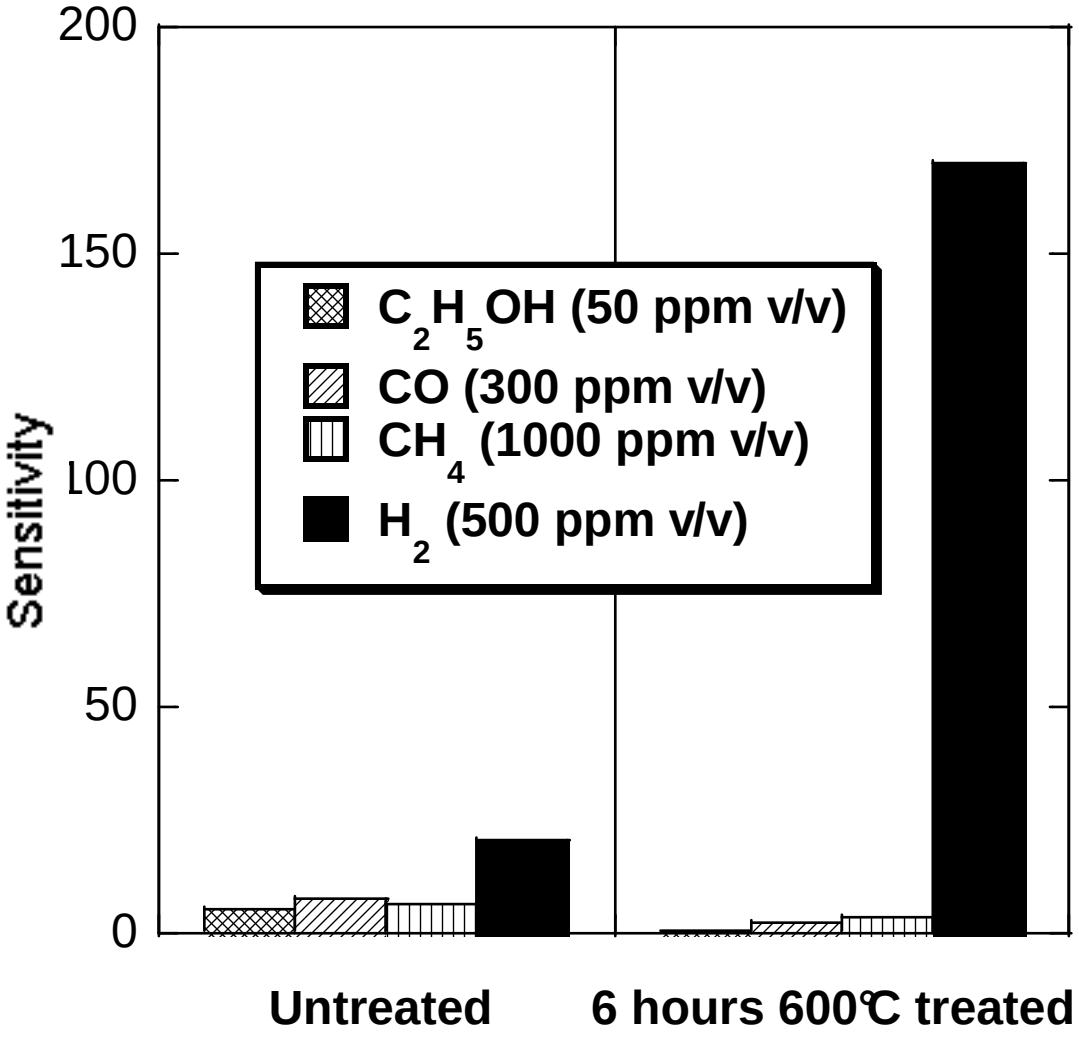
200
150
100
50
0
Sensitivity
C2H5OH (50 ppm v/v)
CO (300 ppm v/v)
CH4 (1000 ppm v/v)
H2 (500 ppm v/v)
Untreated
6 hours 600℃ treated

Fig. 5

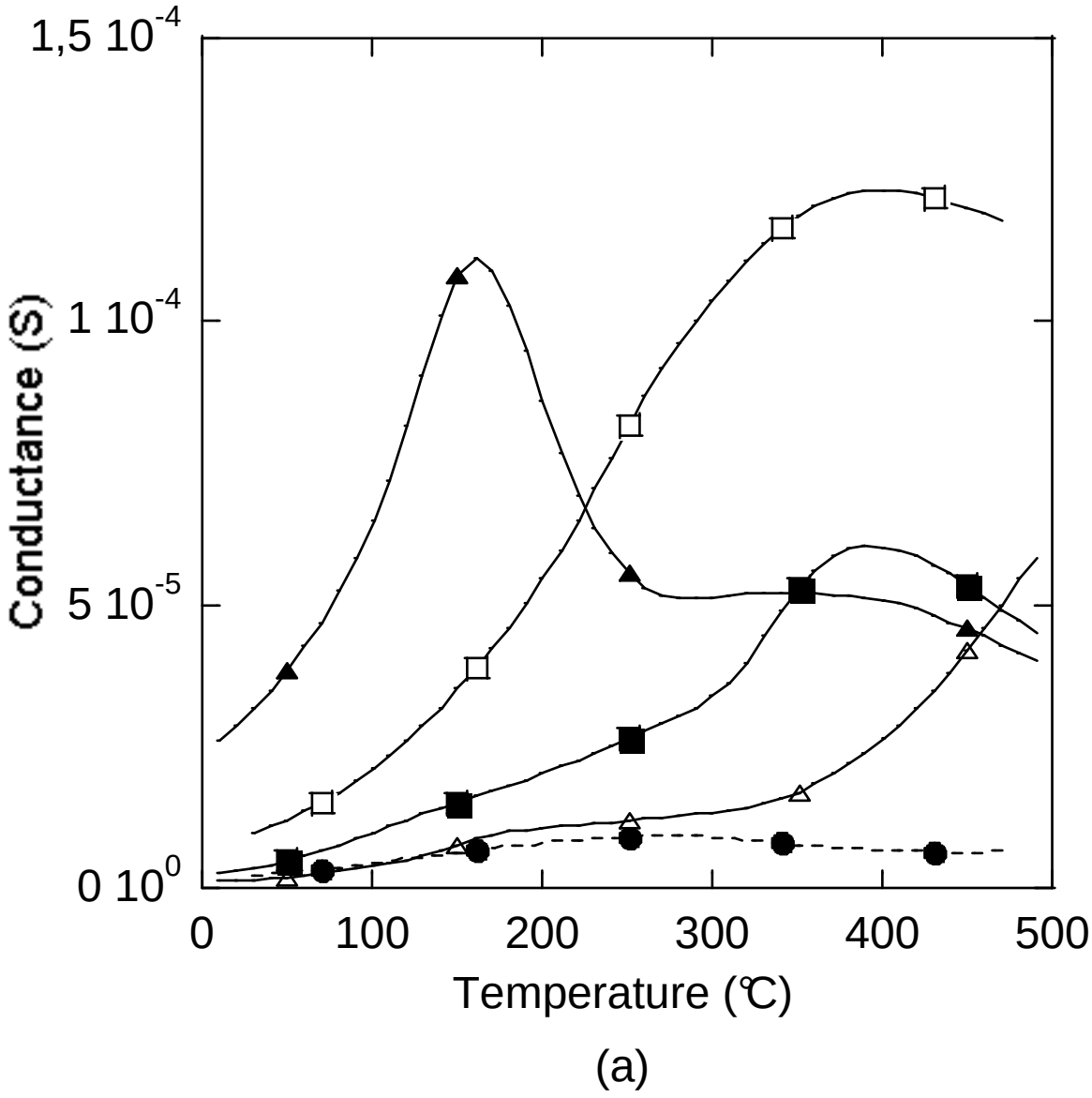
1,5 10-4
1 10-4
5 10-5
0 100
Conductance (S)
0
100
200
300
400
500
Temperature (℃)
(a)

Fig. 6 a

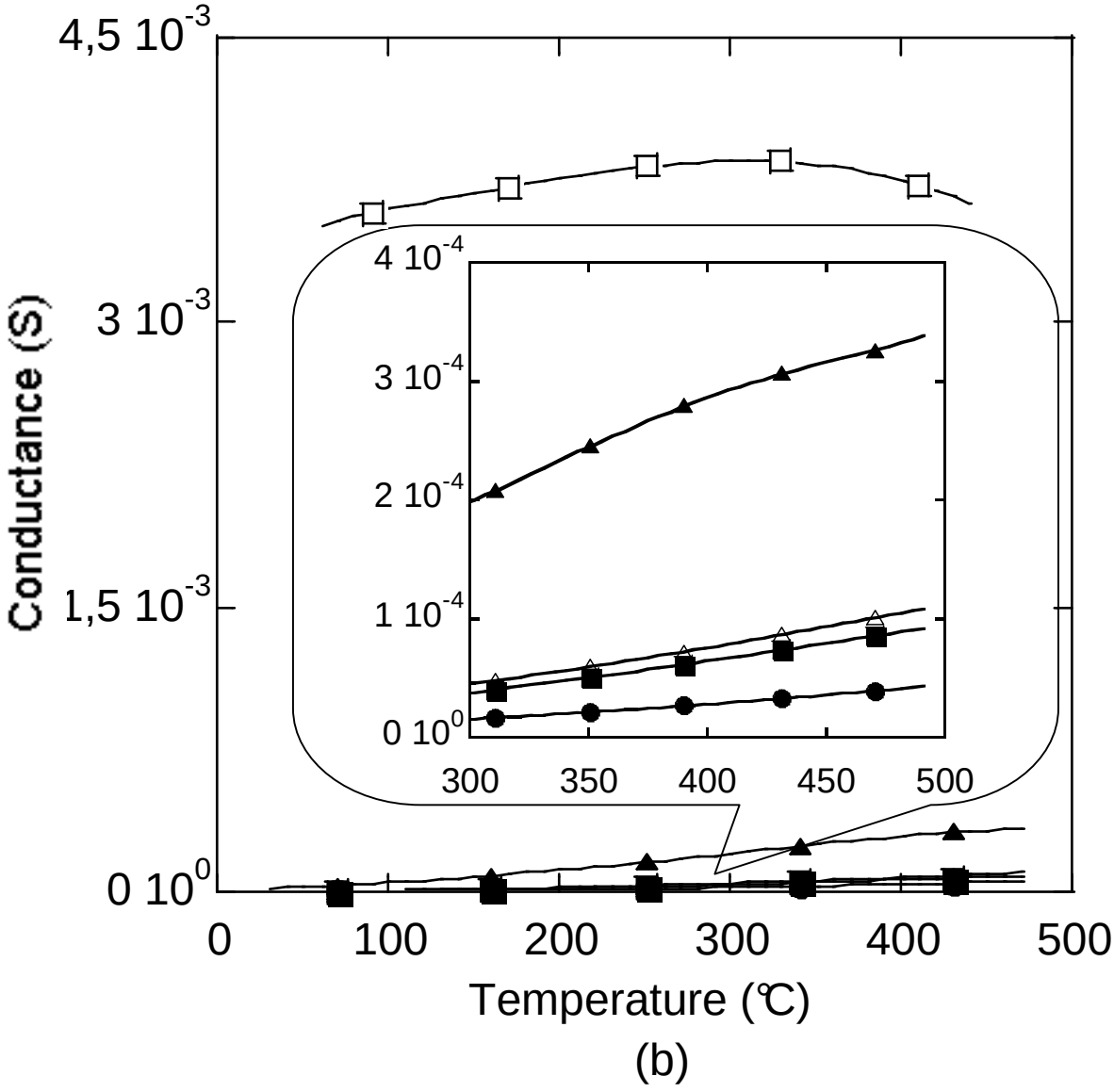
4,5 10-3
3 10-3
1,5 10-3
0 100
Conductance (S)
0
100
200
300
400
500
Temperature (℃)
4 10-4
3 10-4
2 10-4
1 10-4
0 100
300
350
400
450
500
(b)

Fig. 6 b

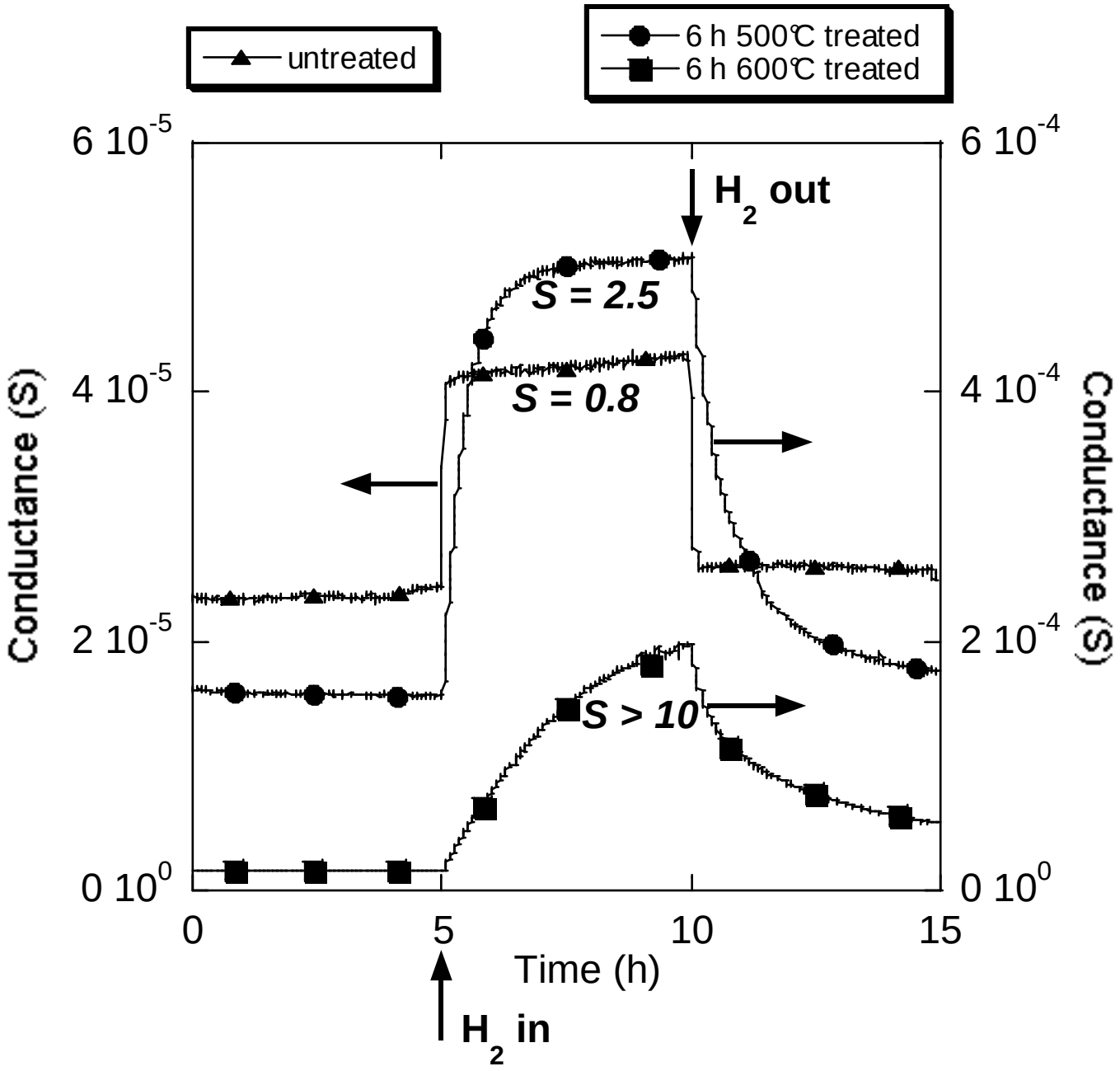
untreated
6 h 500℃ treated
6 h 600℃ treated
6 10-5
4 10-5
2 10-5
0 10^0
6 10-4
4 10-4
2 10-4
0 10^0
Conductance (S)
Conductance (S)
H2 out
S = 2.5
S = 0.8
S > 10
0
5
10
15
Time (h)
H2 in

Fig. 7

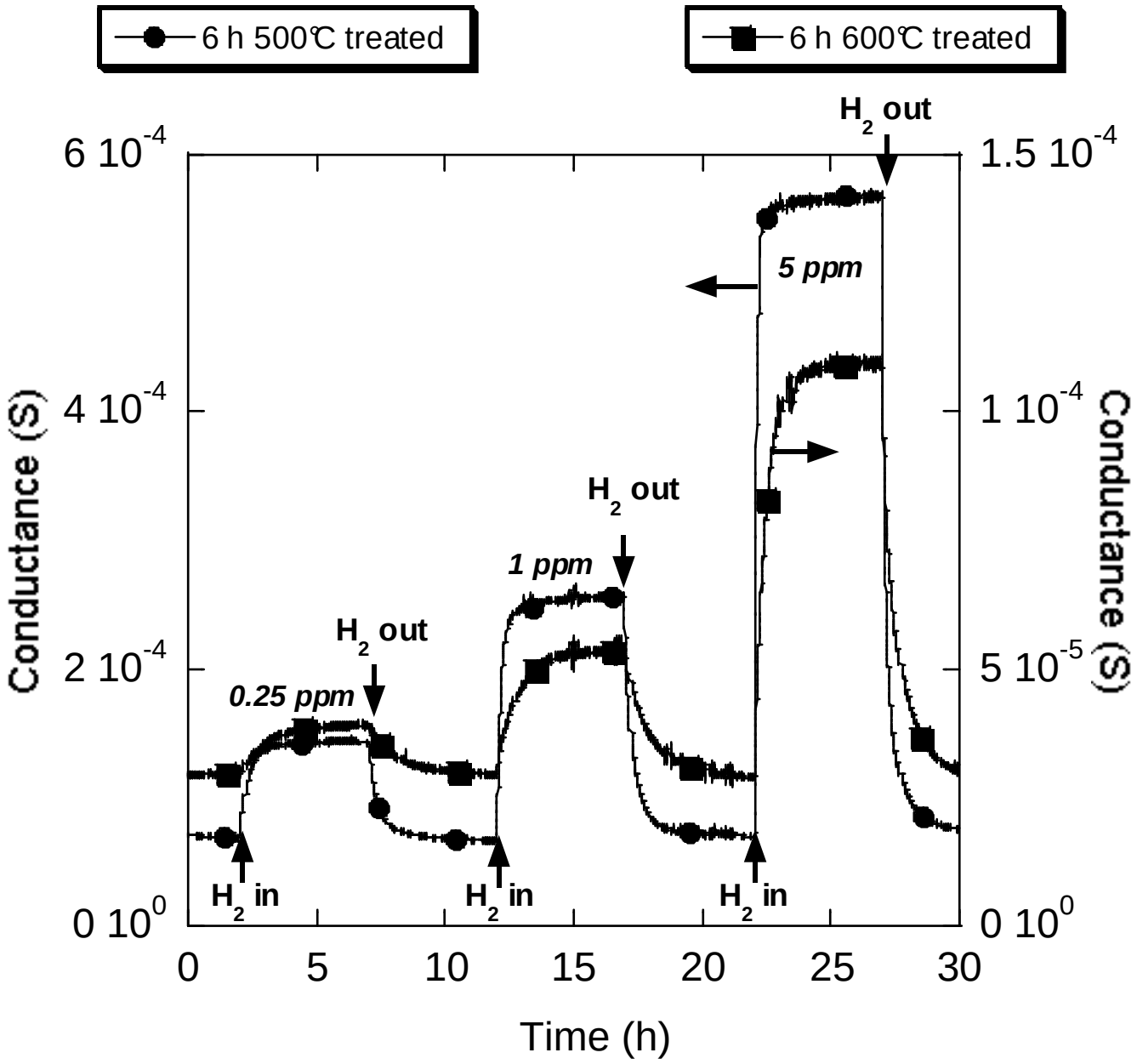
6 h 500℃ treated
6 h 600℃ treated
H2 out
5 ppm
H2 out
1 ppm
H2 out
0.25 ppm
H2 in
H2 in
H2 in
Conductance (S)
Conductance (S)
6 10-4
4 10-4
2 10-4
0 100
1.5 10-4
1 10-4
5 10-5
0 100
0
5
10
15
20
25
30
Time (h)

Fig. 8

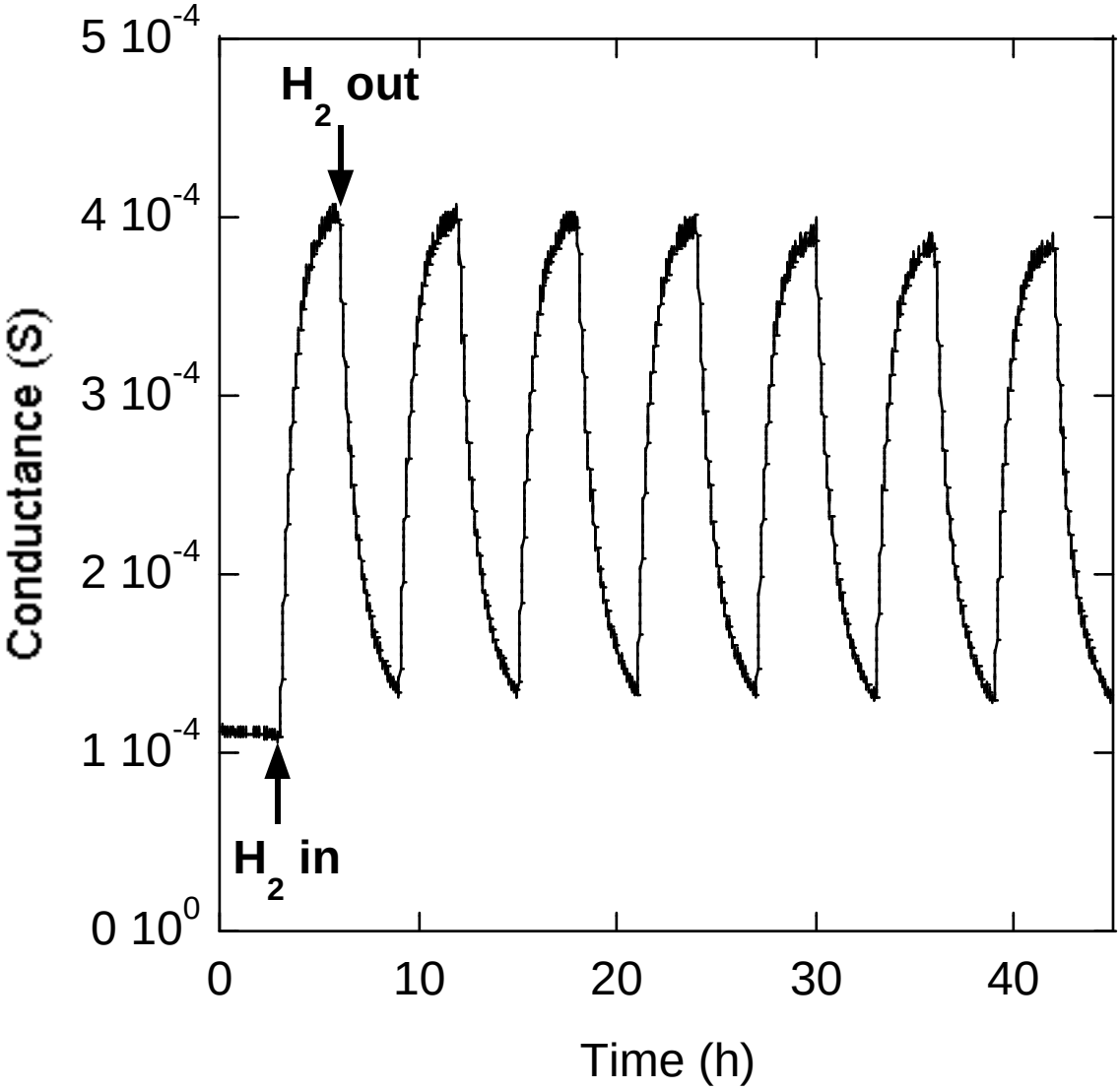
5 10-4
4 10-4
3 10-4
2 10-4
1 10-4
0 100
Conductance (S)
H2 out
H2 in
0
10
20
30
40
Time (h)

Fig. 9

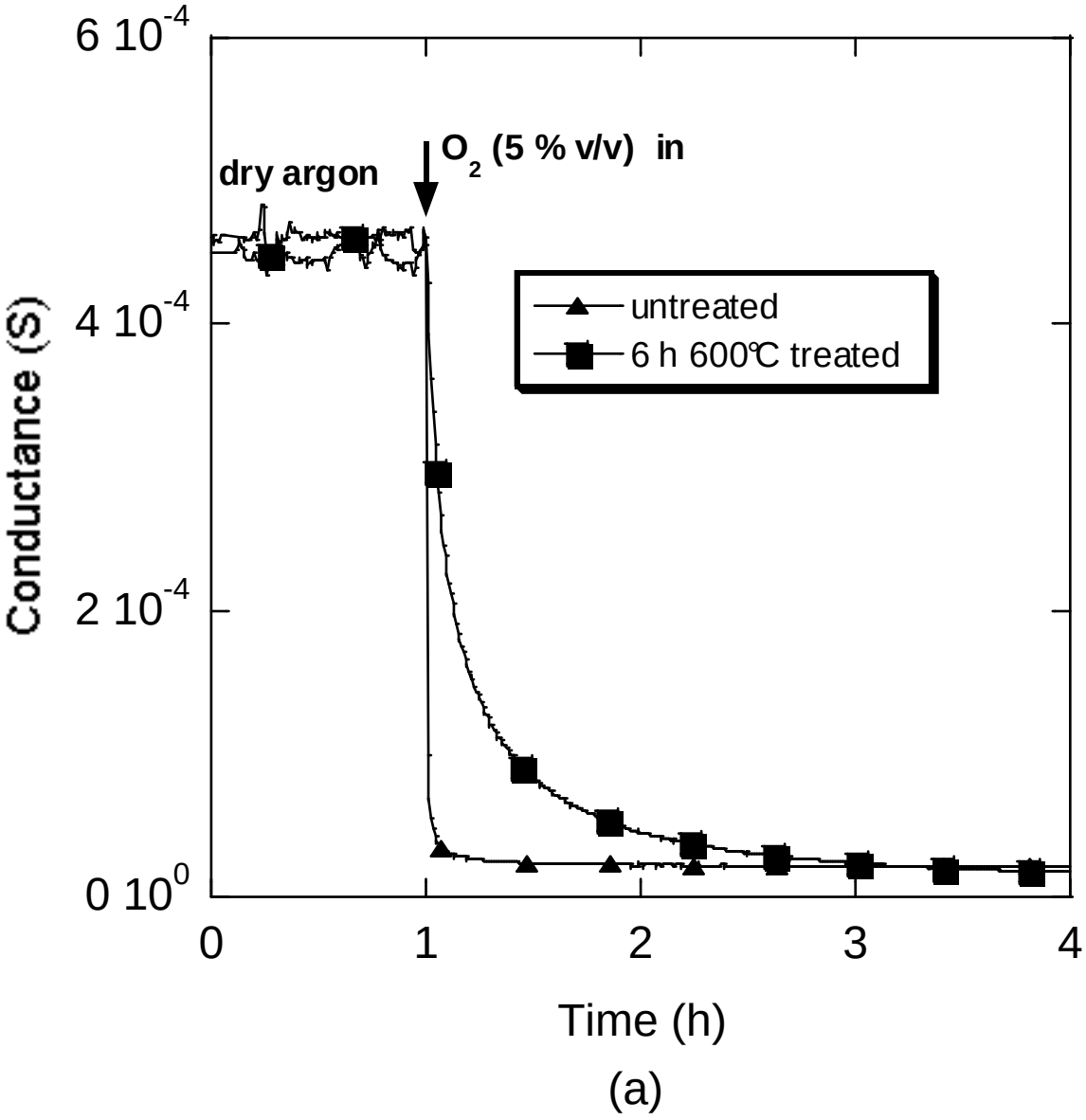
6 10-4
4 10-4
2 10-4
0 100
Conductance (S)
dry argon
O2 (5 % v/v) in
untreated
6 h 600℃ treated
0
1
2
3
4
Time (h)

(a)

Fig. 10 a

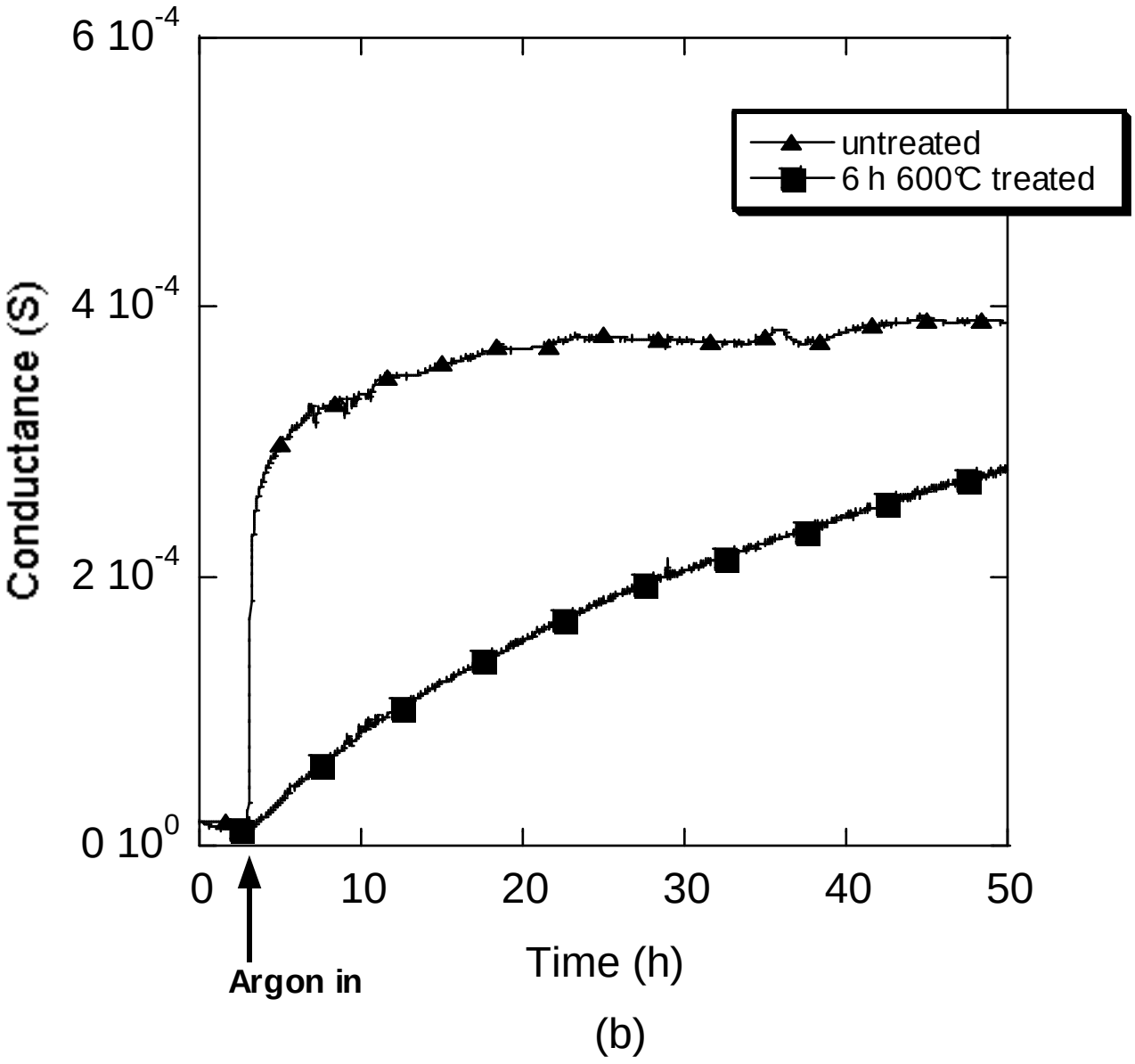
6 10-4
4 10-4
2 10-4
0 10^0
Conductance (S)
untreated
6 h 600℃ treated
0
10
20
30
40
50
Time (h)
Argon in
(b)

Fig. 10 b

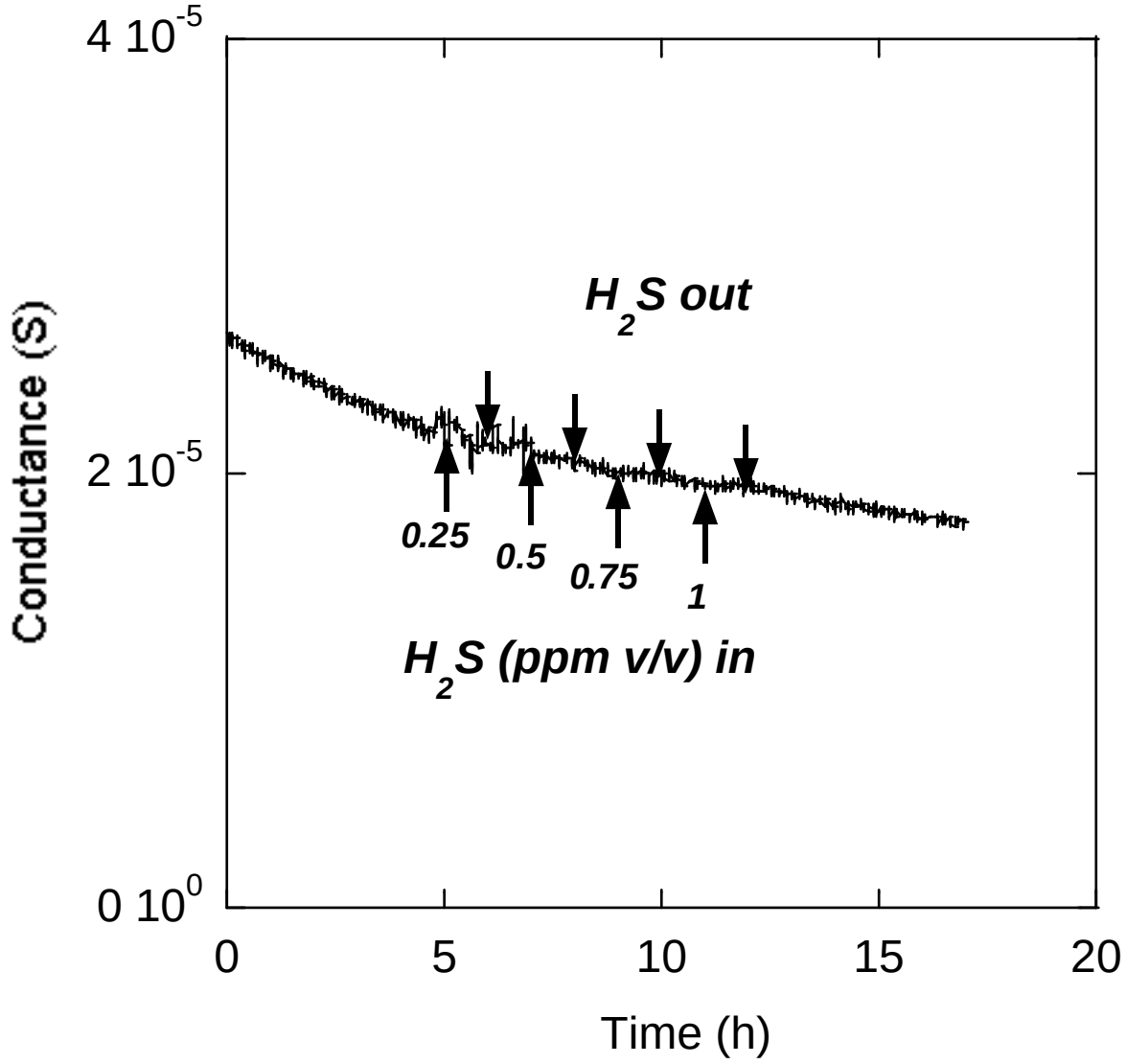
4 10-5
2 10-5
0 100
Conductance (S)
H2S out
0.25
0.5
0.75
1
H2S (ppm v/v) in
0
5
10
15
20
Time (h)

Fig. 11

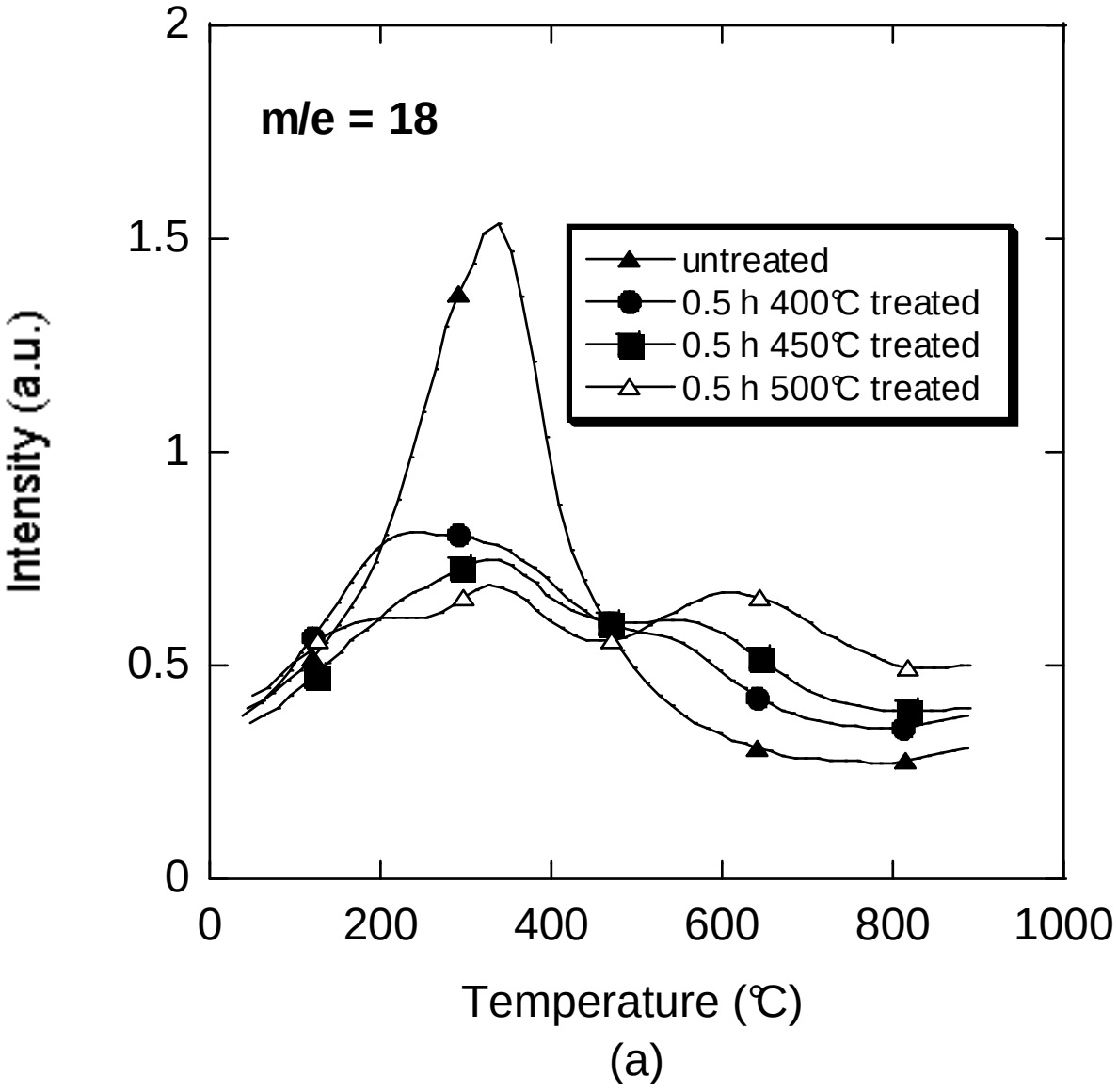
m/e = 18
untreated
0.5 h 400℃ treated
0.5 h 450℃ treated
0.5 h 500℃ treated
Intensity (a.u.)
Temperature (℃)
0
0.5
1
1.5
2
0
200
400
600
800
1000
(a)

Fig. 12 a

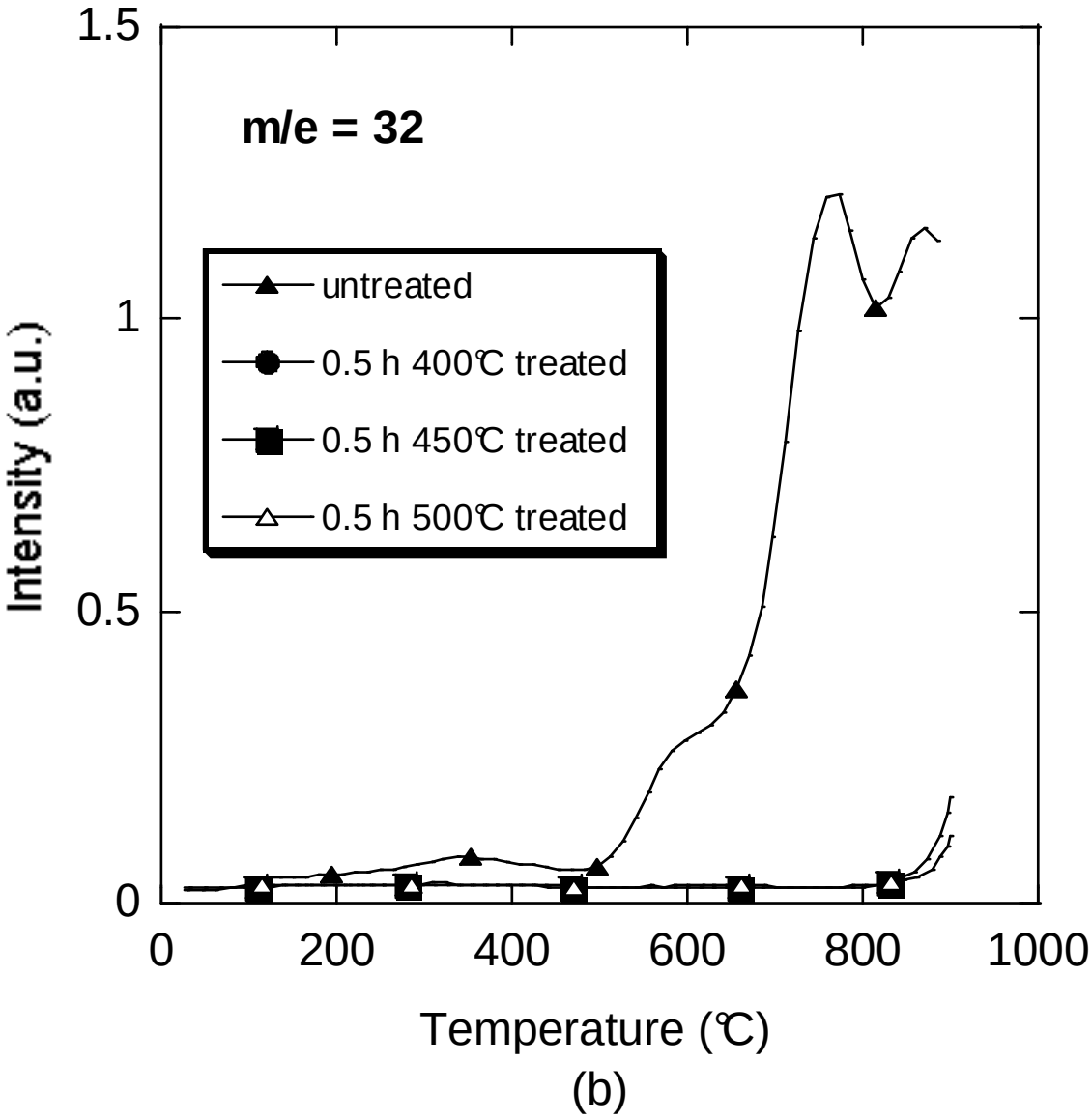
m/e = 32
untreated
0.5 h 400℃ treated
0.5 h 450℃ treated
0.5 h 500℃ treated
Intensity (a.u.)
Temperature (℃)
0
0.5
1
1.5
0
200
400
600
800
1000

(b)

Fig. 12 b

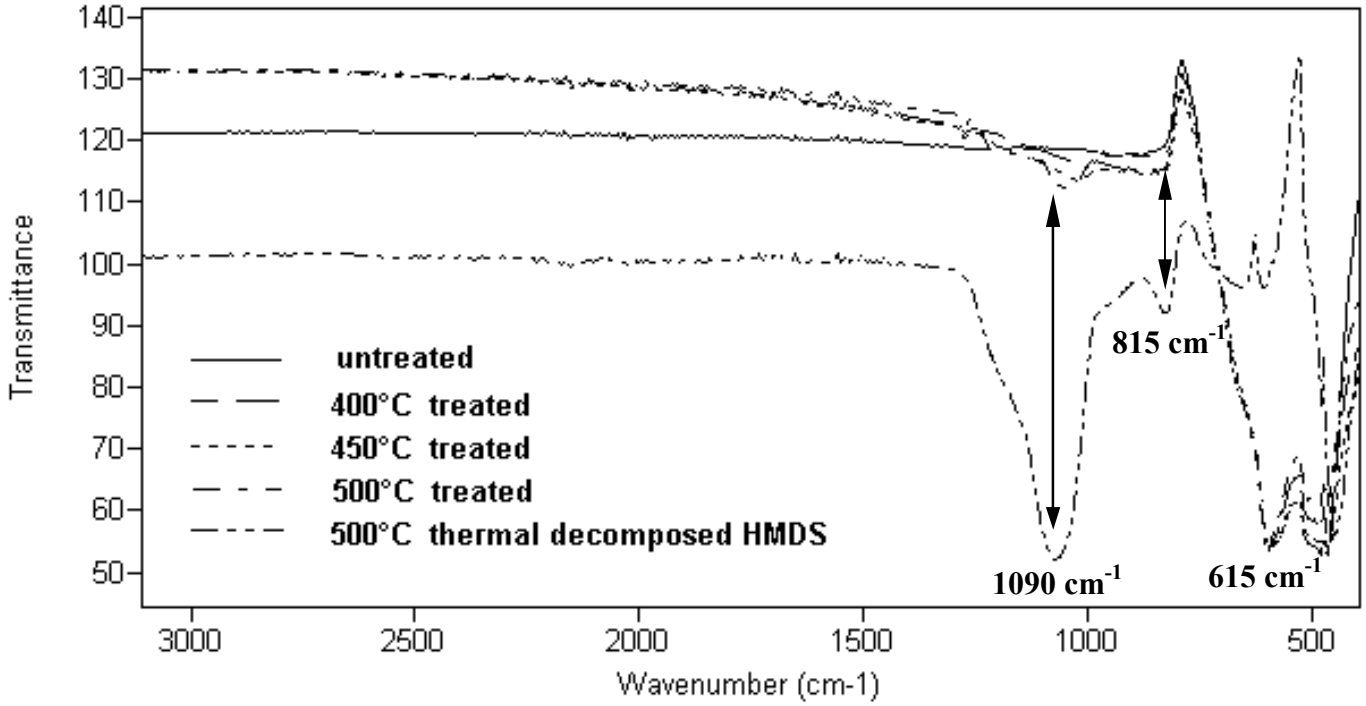
Transmittance
140
130
120
110
100
90
80
70
60
50
3000
2500
2000
1500
1000
500
Wavenumber (cm-1)
untreated
400°C treated
450°C treated
500°C treated
500°C thermal decomposed HMDS
1090 cm-1
815 cm-1
615 cm-1

Fig. 13

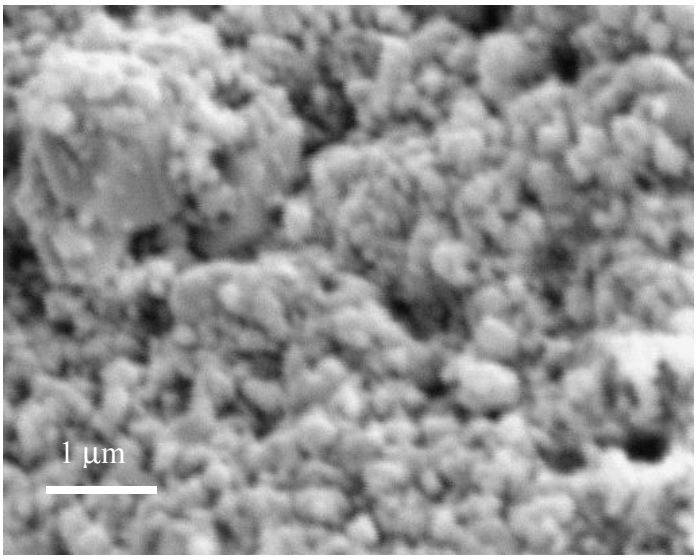

(a)

Fig. 14 a

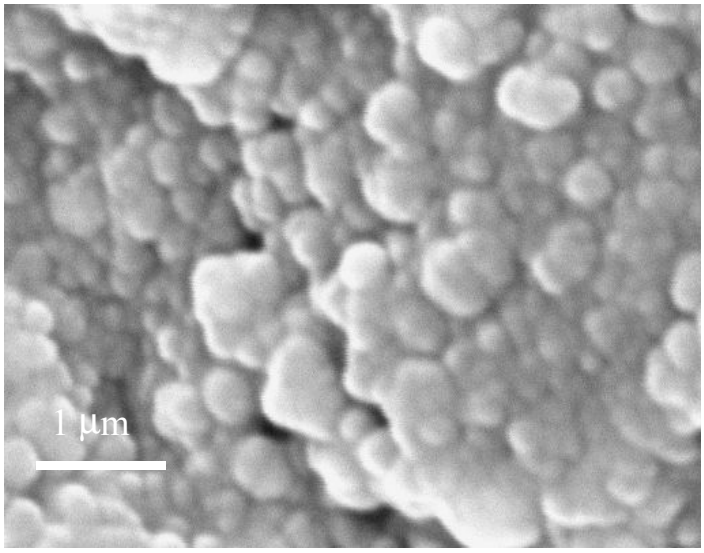

(b)

Fig. 14 b